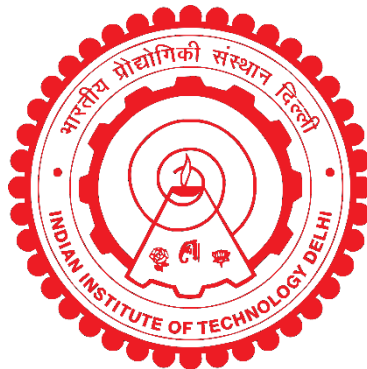


**APPLICATION OF PIEZO SENSORS IN CONDITION
MONITORING OF UNDERGROUND STRUCTURES**

PRATEEK NEGI



**DEPARTMENT OF CIVIL ENGINEERING
INDIAN INSTITUTE OF TECHNOLOGY (IIT) DELHI**

JULY 2018

© Indian Institute of Technology Delhi (IITD), New Delhi, 2018

**APPLICATION OF PIEZO SENSORS IN CONDITION
MONITORING OF UNDERGROUND STRUCTURES**

by

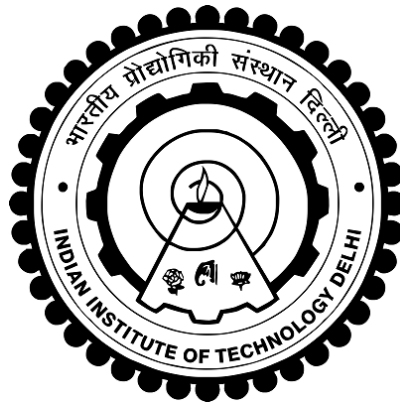
PRATEEK NEGI

Department of Civil Engineering

Submitted

in fulfilment of the requirements of the degree of DOCTOR OF PHILOSOPHY

to the

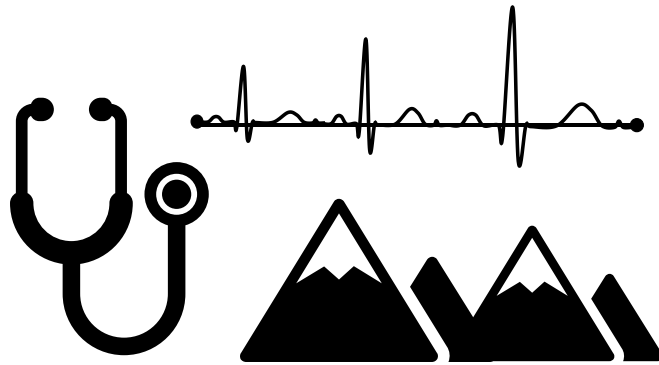


INDIAN INSTITUTE OF TECHNOLOGY (IIT) DELHI

JULY 2018

Dedicated to my family, teachers and friends,

for their support and guidance



CERTIFICATE

This is to certify that the thesis titled “**APPLICATION OF PIEZO SENSORS IN CONDITION MONITORING OF UNDERGROUND STRUCTURES**” which is being submitted by **Mr. PRATEEK NEGI** for the fulfilment of the requirements for the award of the degree of Doctor of Philosophy, is a record of the student’s own work carried out at the **Indian Institute of Technology (IIT) Delhi** under my supervision and guidance. The matter embodied in this thesis has not been submitted elsewhere for the award of any other degree or diploma.

New Delhi
July, 2018

Dr. Tanusree Chakraborty,
Associate Professor
Department of Civil Engineering
Indian Institute of Technology (IIT) Delhi

ACKNOWLEDGMENTS

*First and foremost, I would like to express my deepest gratitude to my guide and mentor **Dr. Tanusree Chakraborty**, who encouraged me to work on an interdisciplinary project. Her continued support and visionary thoughts have been a strong motivation for me. The work ethics and discipline learned from her will help me throughout my academic career.*

*Secondly, I would also like to express a deep sense of gratitude and thankfulness, towards **Prof. Suresh Bhalla**, Department of Civil Engineering, IIT Delhi. His knowledge and support have made this work possible. His resourcefulness and critical reviews have greatly helped me in this work. Besides this, his guidance and knowledge of spirituality and ancient Indian scriptures has nurtured my soul and mind throughout my stay in the campus.*

*A very special thanks to **Dr. Naveet Kaur**, my one and only senior who helped me on every step of my Ph.D. life. She taught me the skills of performing my thought experiments. I feel so blessed to meet her and her husband **Harshdeep Rapal**, who made my weekends relaxing.*

*I am also very thankful towards my friends **Aditya Singh and Ketan Arora**, to help me out in performing my experiments and to discuss my Ph.D. issues. I learned the beauty of working in a research team with them.*

*Also, I would like to thank **Aali Pant, Anuj, Anannya Roy, Durva Gupta, Isha Khanna, Monika Rao, Pawan Kumar, Rajesh Kumar, Riyaz, Roshni Mary, Shivali Chaurasia, Shatakshi Sharma, Sumit Balgavhar, Swapnil Mishra and Sumanth Chinthala** to make all those tea breaks into brainstorming sessions while relaxing in between my strenuous schedule.*

*I am highly indebted to my cycling friends **Khyati Verma, Shabina Ashraf and Aditya Singh**, (who are my family away from home) to give me a new hobby and interest in historical structures.*

*I am also thankful to **Sunita Mishra**, for pointing out all those silly errors in formatting which I could have never pointed out.*

*I would like to thank my **PG Dramatics** family without whom I would have finished my Ph.D. a year ago but, would have missed a wonderful lifetime experience of becoming an actor and assistant director.*

*My thanks are also due to all the civil engineering faculty and other staff members, especially **Mr. Alok Kumar** (Rock mechanics laboratory), **Mr. Lal Singh** (Smart structures and dynamics laboratory), **Mr. Satish** (Civil engineering workshop) for their support and keenness in my work. I am extremely grateful to **Mr. Vinod Sharma** and **Mr. Deepak** (Concrete structural laboratory) to give their helping hand unconditionally, which made my experimentation possible. The kind of cooperation of all those who helped directly or indirectly in the completion of this work is acknowledged herewith.*

*Lastly, I feel privileged and grateful to my parents, **Mrs. Pushpa Negi** and **Col. Jagmohan Negi** and my brother **Prashant Negi** for everything in my life and the fact that I have reached here today. Everything that I have achieved is because of their blessings, encouragement, and support. Thanks to all of you, I really appreciate everything that you have done for me.*

Prateek Negi

ABSTRACT

The underground structures built in rocks are complex in design and require continuous inspection for their maintenance. However, some of the underground areas are inaccessible for the inspection team or might warrant special clearing arrangement, leaving the structure out of service. The complexity of their design, construction and the conditions encountered during service life necessitate the deployment of a dedicated structural health monitoring (SHM) system. It is very crucial to identify the damage in the surrounding rocks in its incipient stage to prevent its further propagation and safeguard the structure built over it. The damage detection in rocks requires an efficient SHM system to monitor the rocks on a regular basis.

At times the stress ratio in the rock due to overburden stress and tectonic activities may reach high value exceeding the threshold, which may lead to rock bursts and subsequent failure of the structure. Besides the static and the quasi-static stresses, cyclic loads acting upon the rocks due to natural or artificial sources lead to deterioration of strength slowly and may result in its fatigue failure. The SHM technique becomes important for underground infrastructure to enable timely detection of the damage caused by any anticipated or unanticipated loads.

In the present study, lead zirconium titanate (PZT) patches are used to monitor the condition of rocks under various forms of loadings using electro-mechanical impedance (EMI) technique. The vibrations generated by the actuation of PZT patch are sensed by the same PZT patch and recorded in the form of conductance and susceptance signatures. The signatures have been quantified using the root mean square deviation (RMSD) method. The study clearly establishes the potential of the EMI technique in detecting and quantifying load induced damages in rocks surrounding the underground structures, opening avenues for applications in real-life situations.

Besides the EMI technique, the same smart sensors are checked for their potential to be used for acoustic emission (AE) monitoring of rocks. The study presents a new simple and cost-effective low-frequency AE technique for monitoring damages in the rocks. The AE technique is demonstrated for monitoring acoustic events happening within the rock specimens under uniaxial compressive loading. Also, the same sensors are used at different orientation positions to monitor the hydration of concrete which is used in the construction of underground structures.

सार

चट्टानों में निर्मित भूमिगत ढांचे डिजाइन में जटिल होते हैं और उनके रखरखाव के लिए निरंतर निरीक्षण की आवश्यकता पड़ती है। हालांकि, कुछ भूमिगत क्षेत्र निरीक्षण टीम के लिए पहुँचने योग्य नहीं होते जिस कारन जांच के समय वो सेवा से बाहर हो सकते हैं। अपने कार्य काल के दौरान उनके डिजाइन, निर्माण और परिस्थितियों में जटिलता को समर्पित संरचनात्मक स्वास्थ्य निगरानी (एसएचएम) प्रणाली की तैनाती की आवश्यकता होती है। अपने प्रारंभिक चरण में आस-पास के चट्टानों में होने वाली क्षति की पहचान करना बहुत महत्वपूर्ण है ताकि इसके आगे के प्रचार को रोकने और उस पर बनाए गए ढांचे की रक्षा की जा सके। चट्टानों में क्षति का पता लगाने के लिए, एक नियमित आधार पर चट्टानों की निगरानी करने के लिए एक कुशल एसएचएम प्रणाली की आवश्यकता होती है। कभी-कभी अतिरंजित तनाव और टेक्टोनिक गतिविधियों के कारण चट्टान में तनाव अनुपात थ्रेसहोल्ड से अधिक मूल्य तक पहुंच सकता है, जिससे चट्टानों के विस्फोट और संरचना की विफलता हो सकती है। स्थिर और अर्ध-स्थैतिक तनाव के अलावा, प्राकृतिक या कृत्रिम स्रोतों के कारण चट्टानों पर चलने वाले चक्रीय भार धीरे-धीरे ताकत में गिरावट का कारण बनते हैं और इसके परिणामस्वरूप स्ट्रक्चर को शती पोहोच सकती है। किसी भी अनुमानित या अप्रत्याशित भार के कारण होने वाली क्षति के समय पर पता लगाने के लिए भूमिगत आधारभूत संरचना के लिए एसएचएम तकनीक महत्वपूर्ण हो जाती है।

वर्तमान अध्ययन में, लीड ज़िकोनियम टाइटेनेट (पीजेडटी) पैच का उपयोग इलेक्ट्रो मैकेनिकल प्रतिबाधा (ईएमआई) तकनीक का उपयोग करके लोडिंग के विभिन्न रूपों के तहत चट्टानों की स्थिति की निगरानी के लिए किया जाता है। पीजेडटी पैच के क्रियान्वयन से उत्पन्न कंपन को एक ही पीजेडटी पैच द्वारा महसूस किया जाता है और आचरण और संवेदना हस्ताक्षर के रूप में दर्ज किया जाता है। हस्ताक्षर को रूट माध्य स्क्रायर विचलन (आरएमएसडी) विधि का उपयोग करके मात्राबद्ध किया गया है। अध्ययन स्पष्ट रूप से भूमिगत संरचनाओं के आसपास चट्टानों में लोड प्रेरित क्षति का पता लगाने और मापने में वास्तविक ईएमआई तकनीक की क्षमता को स्थापित करता है, वास्तविक जीवन स्थितियों में अनुप्रयोगों के लिए मार्ग खोलता है।

ईएमआई तकनीक के अलावा, चट्टानों की ध्वनिक उत्सर्जन (ईई) निगरानी के लिए उपयोग की जाने वाली संभावित क्षमता के लिए एक ही स्मार्ट सेंसर की जांच की जाती है। अध्ययन चट्टानों में क्षति की निगरानी के लिए एक नई सरल और लागत प्रभावी कम आवृत्ति ईई तकनीक प्रस्तुत करता है। ईई तकनीक का प्रदर्शन अनियमित संपीडन लोडिंग के तहत चट्टानों के नमूने के भीतर होने वाली ध्वनिक घटनाओं की निगरानी के लिए किया गया है। साथ ही, भूमिगत संरचनाओं के निर्माण में उपयोग की जाने वाली कंक्रीट की हाइड्रेशन की निगरानी के लिए अलग-अलग अभिविन्यास स्थितियों पर एक ही सेंसर का उपयोग किया गया है।

CONTENTS

Certificate.....	<i>i</i>
Acknowledgement.....	<i>iii</i>
Abstract.....	<i>v</i>
Contents.....	<i>vii</i>
List of figures.....	<i>xi</i>
List of tables.....	<i>xvii</i>
List of symbols.....	<i>xix</i>
List of acronyms.....	<i>xxi</i>
Chapter-1 Introduction.....	1-42
1.1 Introduction.....	1
1.2 Piezoelectricity: The background.....	2
1.3 The piezoelectric effect.....	3
1.3.1 <i>Direct and converse effects</i>	4
1.3.2 <i>Reason for piezoelectric behaviour</i>	5
1.4 Electro-mechanics.....	8
1.5 Dielectric hysteresis and poling of piezoelectric.....	9
1.6 Constitutive relations.....	11
1.7 Computation of strain from voltage output.....	17
1.8 The electro-mechanical impedance technique.....	18
1.8.1 <i>Underlying principle of the EMI method</i>	20
1.8.2 <i>The electro-mechanical admittance</i>	23
1.9 RMSD technique for damage quantification.....	30
1.10 Geotechnical monitoring.....	31
1.10.1 <i>Surface monitoring methods</i>	31
1.10.1.1 <i>Monitoring of surface cracks</i>	31
1.10.1.2 <i>Laser image scanning</i>	32
1.10.1.3 <i>Tiltmeters</i>	33
1.10.1.4 <i>Deformation monitoring using GPS</i>	33
1.10.1.5 <i>Synthetic aperture radar</i>	33
1.10.2 <i>Sub-surface monitoring methods</i>	33
1.10.2.1 <i>Vibrating wire strain gauges</i>	34
1.10.2.2 <i>Measurement of cracks, joints and faults</i>	34
1.10.2.3 <i>Convergence monitoring and surface mounted extensometers</i> ...	35
1.10.2.4 <i>Borehole extensometers</i>	35
1.10.2.5 <i>Ground vibration monitoring</i>	37
1.10.2.6 <i>Borehole inclinometers</i>	38

1.10.2.7	<i>Load cells</i>	39
1.11	Research objectives and scope.....	40
1.12	Organization of the thesis.....	41

Chapter-2 Preliminary experimental and numerical studies of PZT patch and rock interaction..... 43-56

2.1	Introduction.....	43
2.2	Experimental study: Variation of signatures for different bonding stages.....	43
2.3	Numerical study: Finite element (FE) modelling of PZT patch-rock interaction...	49
2.4	Conclusions.....	55

Chapter-3 Damage monitoring of dry and saturated rocks using piezo transducers.. 57-81

3.1	Introduction.....	57
3.2	Need of the study	58
3.3	Instrumentation details and loading sequence	60
3.4	Variation of EMI signatures with damage	63
3.4.1	<i>Dry rock specimen</i>	65
3.4.1.1	<i>Results of first dry specimen</i>	65
3.4.1.2	<i>Results of second dry specimen</i>	68
3.4.1.3	<i>Results of third dry specimen</i>	69
3.4.2	<i>Saturated rock specimen</i>	71
3.4.2.1	<i>Results of first saturated specimen</i>	71
3.4.2.2	<i>Results of second saturated specimen</i>	76
3.4.2.3	<i>Results of third saturated specimen</i>	78
3.5	Conclusions.....	80

Chapter-4 Detection of fatigue in rocks under cyclic stresses using piezo sensors through electro-mechanical impedance technique..... 83-105

4.1	Introduction.....	83
4.2	Need of the study.....	83
4.3	Instrumentation details and loading procedure.....	88
4.3.1	<i>Bonding of PZT patches</i>	88
4.3.2	<i>Experimental setup and loading sequence</i>	90
4.4	Results and discussions.....	94
4.5	Conclusions.....	104

Chapter-5 Cost-effective low frequency acoustic emission (AE) technique for non-destructive examination of rocks using PZT patches..... 107-135

5.1	Introduction.....	107
5.2	Need of the study	107
5.3	Fundamentals of acoustic emission.....	109

5.4	Experimental procedure.....	114
	5.4.1 Specimen preparation.....	114
	5.4.2 Experimental setup and procedure.....	116
5.5	Data processing.....	121
	5.5.1 Cumulative AE counts and event rate.....	121
	5.5.2 Event energy.....	123
5.6	Results and discussions.....	124
5.7	Conclusions.....	134

Chapter-6 Investigations on effectiveness of embedded PZT patches at varying orientations for strain sensitivity and monitoring concrete hydration..... 137-156

6.1	Introduction.....	137
6.2	Need of the study.....	138
6.3	Experimental details.....	140
	6.3.1 Casting of mortar cast.....	140
	6.3.2 Casting of RC beam specimen.....	142
	6.3.3 Acquisition of EMI signatures.....	142
	6.3.4 Setup for strain sensitivity experiment.....	145
6.4	Results and discussions.....	146
	6.4.1 Results of EMI effectiveness study.....	146
	6.4.2 Results of strain sensitivity study.....	154
6.5	Conclusions.....	156

Chapter-7 Conclusions and recommendations..... 157-161

7.1	Introduction.....	157
7.2	Research conclusions and contributions.....	158
7.3	Limitations of using EMI technique for monitoring of rocks.....	160
7.4	Recommendations for future work.....	161

References..... 163-179

Author's publications..... 181-182

Author's curriculum vitae..... 183-185

LIST OF FIGURES

FIGURE	CAPTION	PAGE NO.
1.1	(a) Direct piezoelectric effect in open circuit.....	5
	(b) Direct piezoelectric effect when the circuit is short circuited.....	5
1.2	(a) Inverse piezoelectric effect developing strain, S	6
	(b) Development of stress, F when the movement is stopped.....	6
1.3	The crystal of Lead Zirconium Titanate (PZT)	
	(a) Unit cell is cubic above the curie temperature of 320°C approx...	7
	(b) The unit cell structure is tetragonal below the curie temperature..	7
1.4	Mechanism of poling process.....	8
1.5	Expansion of the polarized piezo ceramic.....	9
1.6	Dielectric hysteresis loop of piezoelectric material.....	9
1.7	Relationships among material properties (Ballato, 1995).....	11
1.8	Tensor directions of PZT patches for constitutive relations	12
1.9	PZT patch taking an EMI signature of the host structure	
	(a) PZT patch bonded on host structure.....	19
	(b) Impedance signature of the damaged and undamaged structure...	19
1.10	Interaction of structural impedance of host structure and electrical impedance of PZT patch (Bhalla, 2004).....	24
1.11	(a) Conductance signature of a PZT patch bonded to a steel structure	29
	(b) Susceptance signature of a PZT patch bonded to a steel structure	29
1.12	(a) Measuring crack distance using steel pins.....	32
	(b) Wire extensometer (Wyllie and Munn, 1979).....	32
1.13	Basic operation of a vibrating wire strain gauge (National Instruments, 2017).....	34
1.14	A digital tape extensometer monitoring tunnel convergence (Sisgeo, 2017).....	36
1.15	A single point and multipoint bore-hole extensometer (Testindo, 2017).....	37
1.16	Principle of Inclinator operations, after Green and Mikkelsen (1988).....	39
1.17	A typical load cell (Tekscan, 2017).....	40
2.1	Complete experimental setup for EMI signature acquisition.....	45
2.2	PZT patch bonded on (a) Kota sandstone and (b) Shiwalik sandstone specimen	46
2.3	Kota sandstone: Conductance signatures at different stages of bonding in (a) 1-300 kHz range (b) 1-120 kHz range.....	47
2.4	Shiwalik sandstone: Conductance signatures at different stages of bonding in (a) 1-1000 kHz range (b) 1-160 kHz range.....	48

FIGURE	CAPTION	PAGE NO.
2.5	Isometric view of PZT bonded on concrete beam and developed von-Mises stresses near the PZT patch modelled in COMSOL...	49
2.6	Comparison of present numerical results with Tseng and Wang (2004) results.....	50
2.7	Isometric view of PZT bonded on the aluminium beam and maximum von-Mises stresses near epoxy and PZT patch interaction modelled in COMSOL.....	51
2.8	Comparison of conductance signature of the present signature with numerical and experimental results (a) Experimental plot by Yang, Lim and Soh (2008) (b) Numerical plot by Yang, Lim and Soh (2008) (c) Numerical plot, present study.....	52
2.9	(a) PZT patch bonded on Kota sandstone cylindrical rock specimen for numerical study.....	53
	(b) von-Mises stresses developed in PZT patch modelled in COMSOL.....	53
2.10	Comparison of conductance signature of the present signature with numerical and experimental results in the range (a) 1 kHz – 1000 kHz (b) 1 kHz – 200 kHz.....	54
3.1	Volumetric compression in rocks under increasing mean stress (Goodman, 1989).....	60
3.2	Cylindrical specimens of Kota sandstone (a) PZT patch bonded at the center of the dry specimen (b) Saturated specimen wrapped in a polyethylene film.....	61
3.3	Experimental setup showing compression testing machine and LCR meter for acquiring EMI signatures.....	63
3.4	Comparison of PZT signatures in free and bonded conditions (a) Conductance signatures (b) Susceptance signatures.....	64
3.5	EMI signatures of first dry rock specimen in the range of 1-1000 kHz (a) Conductance signature (b) Susceptance signature.....	66
3.6	Conductance signature of first dry rock specimen under different loading conditions in the range of 300-500 kHz.....	67
3.7	(a) Histogram showing the variation of RMSD with LR for first dry rock specimen.....	68
	(b) Nonlinear curve fitting for the variation in RMSD with LR.....	68
3.8	Conductance signature of the second dry rock specimen under different loading conditions in the range of 430-470 kHz.....	69
3.9	(a) Histogram showing the variation of RMSD with LR for second dry rock specimen.....	70
	(b) Nonlinear curve fitting for the variation in RMSD with LR.....	70
3.10	Conductance signature of the third dry rock specimen under different loading conditions in the range of 400-540 kHz.....	71

FIGURE	CAPTION	PAGE NO.
3.11 (a)	Histogram showing the variation of RMSD with LR for third dry rock specimen.....	72
(b)	Nonlinear curve fitting for the variation in RMSD with LR.....	72
3.12	EMI signatures of first saturated rock specimen in the complete range of 1 kHz to 1000 kHz corresponding to different load ratios (a) Conductance signature (b) Susceptance signature.....	73
3.13	Conductance signature of first saturated rock specimen under different loading conditions in the range of 320-385 kHz.....	74
3.14 (a)	Histogram showing the variation of RMSD with LR for first saturated rock specimen.....	75
(b)	Non-linear curve fitting for the variation in RMSD with LR.....	75
3.15	Conductance signature of second saturated rock specimen under different loading conditions in the range of 400-600 kHz.....	76
3.16 (a)	Histogram showing the variation of RMSD with LR for second saturated rock specimen.....	77
(b)	Non-linear curve fitting for the variation in RMSD with LR.....	77
3.17	Conductance signature of third saturated rock specimen under different loading conditions in the range of 400-500 kHz.....	78
3.18 (a)	Histogram showing the variation of RMSD with load ratio LR for third saturated rock specimen.....	79
(b)	Non-linear curve fitting for the variation in RMSD with LR.....	79
4.1	Influence of cyclic stress variation at frequency 20 Hz on strain variation as a function of time (Attewell and Farmer, 1973).....	85
4.2	(a) Specimen bonded with PZT patch (b) Soldered terminals on the PZT patch.....	89
4.3	Complete experimental setup showing cyclic loading machine and EMI data acquisition system in IIT Delhi.....	90
4.4	(a) Cyclic loading at 4 Hz (b) typical stress-strain curve achieved for first 1000 cycles, specimen N3.....	92
4.5	Failed specimen after cyclic testing of Kota sandstone specimen (N1).....	93
4.6	Conductance signatures of specimen N1 in the range of (a) 1-300 kHz (b) 45-150 kHz.....	98
4.7	Conductance signatures of specimen N2 in the range of (a) 1-300 kHz (b) 100-135 kHz.....	99
4.8	Conductance signatures of specimen N3 in the range of (a) 1-300 kHz (b) 70-125 kHz.....	100
4.9	Conductance signatures of specimen N4 in the range of (a) 1-300 kHz (b) 75-85 kHz.....	101
4.10	Conductance signatures of specimen N5 in the range of (a) 1-300 kHz (b) 65-85 kHz.....	102

FIGURE	CAPTION	PAGE NO.
4.11	Sub root mean square deviations in conductance signature after subsequent number of load cycles for rock specimens (a) N1 (b) N2 (c) N3 (d) N4 (e) N5.....	104
5.1	Frequency ranges for various AE and other related studies (Hardy, 1972.....	112
5.2	(a) PZT patch bonded on the rock specimen.....	115
	(b) An ESG bonded on the other side of the specimen.....	115
	(c) Cross-section of bonded PZT patch.....	115
5.3	The complete experimental setup for recording acoustic emissions (AE)	117
5.4	Schematic diagram of AE recording system used in the present study.....	118
5.5	A typical laboratory AE recording system (Ishida et al., 2017)...	118
5.6	Pencil lead breaker (PLB) test for the present AE system (a) Event recorded in time domain and (b) frequency domain.....	120
5.7	A typical AE event and illustration for energy calculations (GOI Ministry of Railways 2009, ASTM 2009)	122
5.8	Acquired AE signature of (a) specimen 0.01A with very less noise level and (b) specimen 0.01B with higher noise level.....	123
5.9	FFT plots of acquired AE signatures of all the rock specimens (a) 0.1A (b) 0.1B (c) 0.1C (d) 0.05A (e) 0.05B (f) 0.05C (g) 0.01A (h) 0.01B (i) 0.01C.....	125
5.10	Cumulative AE count plots and relative energy plots for the specimens tested at 0.01 mm/s displacement rate (a) AE counts of specimen 0.01A (b) Relative energy plot of specimen 0.01A (c) AE counts of specimen 0.01B (d) Relative energy plot of specimen 0.01B (e) AE counts of specimen 0.01C (f) Relative energy plot of specimen 0.01C.....	126
5.11	Cumulative AE count plots and relative energy plots for the specimens tested at 0.05 mm/s displacement rate (a) AE counts of specimen 0.05A (b) Relative energy plot of specimen 0.05A (c) AE counts of specimen 0.05B (d) Relative energy plot of specimen 0.05B (e) AE counts of specimen 0.05C (f) Relative energy plot of specimen 0.05C.....	127
5.12	Cumulative AE count plots and relative energy plots for the specimens tested at 0.1 mm/s displacement rate (a) AE counts of specimen 0.1A (b) Relative energy plot of specimen 0.1A (c) AE counts of specimen 0.1B (d) Relative energy plot of specimen 0.1B (e) AE counts of specimen 0.1C (f) Relative energy plot of specimen 0.1C.....	128

FIGURE	CAPTION	PAGE NO.
5.13	Event rate plots for specimens tested at 0.01 mm/s displacement rate (a) Event rate for specimen 0.01A (b) Event rate for specimen 0.01B (c) Event rate for specimen 0.01C.....	130
5.14	Event rate plots for specimens tested at 0.05 mm/s displacement rate (a) Event rate for specimen 0.05A (b) Event rate for specimen 0.05B (c) Event rate for specimen 0.05C.....	131
5.15	Event rate plots for specimens tested at 0.1 mm/s displacement rate (a) Event rate for specimen 0.1A (b) Event rate for specimen 0.1B (c) Event rate for specimen 0.1C.....	132
6.1	(a) PZT patches bonded on the cement mortar casting.....	141
	(b) Embedded completely in the cuboid mortar cast.....	141
6.2	Casting of the RC beam and placement of the mortar cuboid over the top reinforcement.....	143
6.3	Schematic diagram of the experimental setup for EMI acquisition.....	144
6.4	Sub-frequency distribution of conductance signature on 3 rd day of curing of the beam.....	144
6.5	Complete experimental setup for excitation of beam and voltage measurement from the embedded piezo sensors.....	145
6.6	EMI signatures of vertically (90°) oriented PZT patch in all sub-frequency ranges.....	148
6.7	EMI signatures of inclined (45°) oriented PZT patch in all sub-frequency ranges.....	149
6.8	EMI signatures of horizontally (0°) oriented PZT patch in all sub-frequency ranges.....	150
6.9	RMSD plots with 3 rd day signature as the base line for (a) Vertical (90°) (b) Inclined (45°) and (c) Horizontal (0°) PZT patches.....	152
6.10	RMSD plots with the preceding day as the base line for (a) Vertical (b) Inclined and (c) Horizontal PZT patches.....	153
6.11	Comparison of FFT Voltages with different excitation frequencies for different PZT positions at (a) 0.25L and (b) 0.50L of the beam.....	154

LIST OF TABLES

TABLE	CAPTION	PAGE NO..
1.1	Properties of PZT at room temperature after poling (Jaffe et al., 1954).....	4
1.2	Different piezoelectric parameters.....	14
2.1	Physical and mechanical properties of Kota and Shiwalik sandstones.....	44
2.2	PIC-151 material and araldite epoxy technical data (Araldite 2017; PI ceramic 2017).....	44
3.1	Physical and mechanical properties of Kota sandstone.....	61
4.1	Details of testing conditions of different specimens.....	93
4.2	S-RMSD variation in all the specimens in different frequency ranges.....	95
6.1	Properties of the RC beam.....	142
6.2	RMSD % values of PZT patches with 3 rd day signature as the base line placed at (a) vertical (b) inclined and (c) horizontal direction.....	147

LIST OF SYMBOLS

A	Force required to produce a unit velocity in the PZT patch
B	Susceptance
C_p	Capacitance of the sensor
C_0	Static capacitance for a square PZT patch of size l
D	Electric displacement
$[D_m]$	Electric displacement vector
$[d_{jm}]$	Third order piezoelectric strain coefficient tensors for direct piezoelectric effects
$[d_{mj}]$	Third order piezoelectric strain coefficient tensors for converse piezoelectric effects
d_{31}	Piezoelectric strain coefficient
$d_{ij}, e_{ij}, g_{ij}, h_{ij}$	Constants for describing piezoelectricity
dA_1, dA_2, dA_3	Area of electrodes in the 2-3, 1-3 and 1-2 planes respectively
E	External field/ Electric field
$[E]$	Applied external electric field
E_{dry}	Dry elastic modulus of rock
F	Force
f_{ck}	Characteristic strength of concrete
G	Conductance
G_j^1	Post-damage conductance at the j^{th} frequency point
G_j^0	Conductance value pertaining to the pristine state at the j^{th} frequency point
G_s	Specific gravity of rock
j	Unit imaginary number
k	Electro-mechanical coupling factor
k_n, K	Wave number
L/D	Length to diameter ratio
l_s	Half-length of sensor
m	Mass per unit length
P_r	Remanent polarization
P	Polarization
q	Charge
S	Strain
S_1	Strain in direction-1 (x)
$[S_{ji}^E]$	Fourth order elastic compliance tensor under constant electric field
$[S_j]$	Second order strain tensor
s_{km}^E	Elastic compliance
T	Mechanical stress

$[T]$	Stress tensor
T_1	Axial stress in direction-1 (x)
t_s	Thickness of sensor
t_r	Time of rise
t	Time
$\tan \delta$	Dielectric loss factor of the PZT material
\dot{u}	Velocity response
u	Displacement in the piezo patch in direction-1 (x) at time t
V	Voltage
V_s	Developed voltage
w_s	Width of sensor
\bar{Y}	Electromechanical admittance
Y_s	Young's modulus of the piezoelectric material
\bar{Y}^E	Complex Young's modulus of elasticity of the PZT patch
Z_E	Electrical impedance
Z_T, Z_a	Mechanical impedance of the piezoelectric patch
Z_s, Z	Mechanical impedance of the host structure
β	Damping ratio
ϵ	Dielectric constant
ϵ_0	Permittivity of free space equal to 8.854×10^{-12} F/m
ϵ_T	Permittivity for free condition
ϵ_s	Permittivity for fixed condition
ϵ_{km}^E	Dielectric permittivity
ω	Angular frequency
$\bar{\epsilon}_{33}^T$	Complex electric permittivity in direction-3 (z) of the piezo material at constant stress
η	Mechanical loss factor of the PZT material
ρ	Density of the patch
ρ_{dry}	Dry density of rock
ρ_{sat}	Saturated density of rock
σ_c	Unconfined compressive strength of rock
μ_{dry}	Dry Poisson's ratio of rock
ϕ_{true}	True porosity

LIST OF ACRONYMS

AE	Acoustic Emission
CCD	Correlation Coefficient Deviation
CTM	Compression Testing Machine
EMI	Electro Mechanical Impedance
ESG	Electrical Strain Gauges
FFT	Fast Fourier Transformation
FBG	Fiber Bragg Grating
FE	Finite Element
H-N	Hsu-Neilson
LCR	Inductance Capacitance Resistance
LR	Load Ratio
LEFM	Linear Elastic Fracture Mechanics
MAPD	Mean Absolute Percentage Deviation
MIT	Mechatronic Impedance Transducer
NDT	Non-Destructive Testing
NDE	Non-Destructive Evaluation
PC	Personal Computer
PLB	Pencil-Lead Breakage
PZT	Lead Zirconate Titanate
RMSD	Root Mean Square Deviation
RC	Reinforced Concrete
RD	Relative Deviation
SNR	Signal to Noise Ratio
SHM	Structural Health Monitoring
S-RMSD	Sub-Root Mean Square Deviation
UCS	Unconfined Compressive Strength